STUDIES OF MAGNETOSTATIC AND MAGNETORESONANCE PROPERTIES OF $La_{0.7}Sr_{0.3}MnO_3$ NANOPOWDERS

O.V. BONDAR, V.M. KALITA, A.F. LOZENKO, D.L. LYFAR, S.M. RYABCHENKO, P.O. TROTSENKO, I.A. DANILENKO[1]

Institute of Physics, Nat. Acad. Sci. of Ukraine
(46, Nauky Ave., Kyiv 03028, Ukraine),

[1]**Donetsk Physical & Technical Institute, Nat. Acad. Sci. of Ukraine**
(72, R. Luxembourg Str., Donetsk 83114, Ukraine)

UDC 539

Investigations of magnetostatic and magnetoresonance (EPR, FMR, NQR/NMR) properties of $La_{0.7}Sr_{0.3}MnO_3$ manganite nanoparticles with a linear size of 50–200 nm have been carried out. It has been shown that samples are magnetized similarly to multidomain ferromagnets and demonstrate hysteresis loops within the whole temperature range where the ferromagnetic phase exists. At the same time, the transformation of the multidomain state of a sample to a uniform one is caused by the reorientation of the magnetic moments of unidomain particles. The temperature behavior of the magnetic susceptibility of the sample in the magnetically ordered state is similar to that for superparamagnets. Such a character of the sample magnetization corresponds to the change of the latter due to the thermally activated reorientations of magnetic moments of individual unidomain nanoparticles. It is also in agreement with the presence of an additional absorption peak in the ferromagnetic resonance spectrum, which has been revealed in a narrow range in the vicinity of the zero field, where the reorientation of the magnetic moments of nanoparticles takes place. Some differences between the magnetization peculiarities of the samples fabricated by the mechanical pressing of nanoparticles and those where the particles were in the powder state have been revealed. Manifestations of both the superparamagnetism of individual nanoparticles and the influence of the dipole-dipole interaction between closely located particles in the ensemble have been observed in $La_{0.7}Sr_{0.3}MnO_3$ nanopowders while analyzing the NQR/NMR signal of ^{139}La nuclei in the internal field of ferromagnetic samples. We guess that, owing to such an interaction, closely located unidomain particles form many-particle conglomerates bound by magnetic ponderomotive forces.

1. Introduction

A growth of attention to the studying of $Re^{(3)}_{1-x}Me^{(2)}_xMnO_3$ manganites, where trivalent rare-earth ions, $Re^{(3)}$, are substituted partially by bivalent metal ones, $Me^{(2)}$ (see, e.g., review [1]), is caused first of all by the phenomenon of colossal magnetoresistance inherent to them. This phenomenon manifests itself mainly in the range of temperatures below the temperature of the paramagnetic insulator–ferromagnetic metal phase transition which occurs in the electron systems of those substances. The transition temperature depends on the degree of substitution x and the types of both the rare-earth ions and the ions which replace them. Perspective for applications are the nanofilms and magnetic coatings consisting of nanoparticles of materials possessing colossal magnetoresistance.

Ferromagnetic particles, the linear size of which is of the order of or less than 10–50 nm, are known to have a unidomain structure [2]. If the barrier for the magnetic moment reorientation between the equivalent directions of "easy" magnetization should exceed the actual temperature T (the latter is measured in energy units), the coercive force for remagnetization of such particles will be maximally possible. Provided the reciprocal relation between the barrier and the temperature value, particles will behave as superparamagnetic ones [2]. Superparamagnetism will manifest itself in the properties of the many-particle system if unidomain ferromagnetic nanoparticles are located at rather large distances from one another, so that the dipole-dipole interaction between them can be neglected. But if nanoparticles are closely packed, the dipole magnetic fields of separate particles will "block" mutually the reorientation of magnetization directions by one another, and the system behavior will be similar to the properties of a massive polycrystalline ferromagnet with nanosized grains. The study of magnetostatic and magnetoresonance properties of manganite nanoparticles, as well as the peculiarities of their manifestation related to the interaction between the particles of the samples under consideration, was the main topic of investigations in this work.

2. Samples under Consideration

The magnetic and magnetoresonance properties of $La_{0.7}Sr_{0.3}MnO_3$ nanoparticles 50—200 nm in dimension

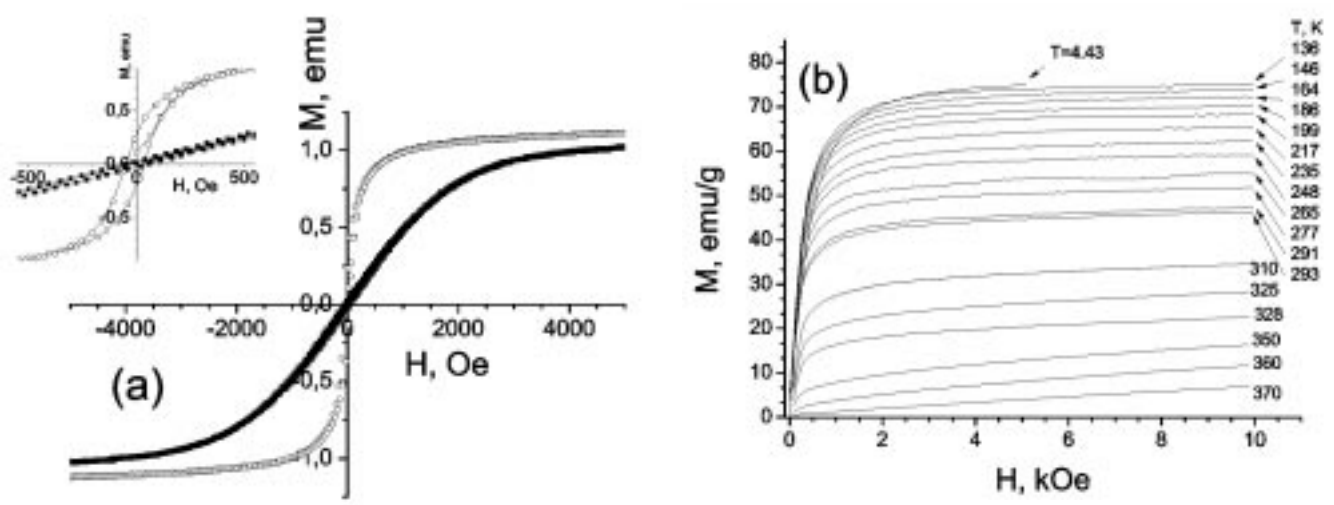

Fig. 1. *a* — Magnetization curves for $La_{0.7}Sr_{0.3}MnO_3$ obtained at $T = 293$ K. The field was directed transversely to (open circles) or along (solid squares) the disk-like (tablet) sample axis. The central parts of the plots are shown scaled up in the inset to make the hysteresis loops noticeable. *b* – Magnetization curves obtained at various temperatures for the field oriented in the plane of the tablet

were studied. Particles with a definite size were separated taking advantage of the rate of their precipitation in a liquid (see the description of technology in [3]). The form of the particles was not monitored.

Our samples consisted of particles, the size of which was close to the threshold of the unidomain state. Owing to the dispersion of the particle sizes, some of the particles had to be unidomain. The others can be made up of a few domains. Therefore, if the magnetic fields created mutually by particles, which were closely packed within the samples, did not result in a reciprocal "blocking" of the magnetization directions in individual particles, one might expect that the phenomena similar to superparamagnetism would manifest themselves in the magnetic properties of the samples under consideration. Moreover, taking the dense packing of particles into account, one might expect that the interparticle interaction would manifest itself.

In order to study the magnetostatic properties, we used the samples fabricated in the form of thin disks about 0.3 mm in thickness and about 5.0 mm in diameter. They were fabricated by pressing the powder of 50–100-nm nanoparticles with the application of minimal efforts. The particles were not destroyed and did not penetrate into one another under the pressure, but stuck together, keeping the tablet form. They cannot rotate more with respect to one another under the action of a magnetic field. The average density of a sample fabricated in such a manner was approximately 4.25 g/cm^3. The relative "factor of nanoparticle packing" in a tablet was about 60%. In addition, several samples were fabricated of a powder with the grains 100–200 nm in size. The powder was poured into a tank, whose form was close to the cubic one, and sealed by a wad of cotton wool. Some individual particles in the tank might probably rotate under the action of an external field.

In order to study the electron spin resonance (EPR/FMR), a small amount (up to 1–1.5 mg) of the powder of 100—200-nm nanoparticles was put without special fixation onto the bottom of an ampoule with the internal diameter of about 1.5 mm. At the same time, to study the nuclear quadrupole (NQR) and nuclear magnetic (NMR) resonances in the internal field of the ferromagnetic sample, the similar nanoparticles (100—200 nm in size) were placed into an ampoule 5 mm in diameter and about 40 mm in length. In this case, the dipole-dipole interaction of the particles would also affect the magnetic properties of the sample as a whole. The action of the magnetic forces can induce the relative turns of the particles.

3. Magnetostatic Measurements

Magnetostatic measurements were carried out using an LDJ-500 vibromagnetometer in the temperature range 4.2—400 K. The dependences of the magnetic moment M of a 25-mg sample consisting of pressed $La_{0.7}Sr_{0.3}MnO_3$ particles on the magnetic field H at $T = 293$ K are exhibited in Fig. 1, *a*. At this temperature, the

particles are ordered ferromagnetically. Presented in the figure are the data for two experimental setups, where the magnetic field was directed along (solid squares) and across (open circles) the axis of the disk-like tablet. In both cases, the hysteresis was observed, and the sample behaved as a multidomain ferromagnet. The observed anisotropy of the sample magnetization corresponded to what might be expected in the case of the magnetically isotropic material of the tablet and provided that the anisotropy of the sample form gave the main contribution to the magnetic anisotropy of the whole sample. As is follows from the magnetization curve that corresponds to the orientation of the magnetic field across the tablet axis, the saturation of the sample magnetic moment was observed at the field that was not larger than 0.75–1 kOe. This means that the intrinsic anisotropy of the particles is small, and the anisotropy fields in them do not exceed 1 kOe. The manifestation of hysteresis and the residual magnetization evidence for a partial irreversibility of the rearrangement of magnetic domains (or, to put it more precisely, the magnetic moments of individual particles) within the sample. The measurements carried out in the temperature range from 4.2 to 400 K testify to that a similar magnetization behavior takes place in the whole interval $T < T_C$, where $T_C = 360$ K is the Curie temperature. In this temperature range, the magnetization curves correspond to the easy-plane anisotropy of the investigated disk made up of nanoparticles. The magnetization hysteresis is observed in the whole range of ferromagnetic ordering. The value of T_C quoted above was determined from the temperature and field dependences of magnetization. The same value is obtained when analyzing the temperature transformations of the EPR spectra.

The set of magnetization curves of the same sample measured at various temperatures and for the magnetic field directed in the disk plane is shown in Fig. 1,*b*. One can see that at every temperature, the corresponding curve, after a drastic slowing down of its initial steep growth, demonstrates a rather weak further growth of the magnetization, which is quasi-linear in the field in a wide enough field range (partial saturation). The magnetization saturation for comparatively small fields is typical of multidomain ferromagnets, where the basic mechanism of growth of the magnetization M in an increasing magnetic field comprises the motion of the domain boundaries and the corresponding increase of the total volume of those domains, whose magnetizations are aligned along the field. At $T \neq 0$, this saturation is not complete. As the field increases further, the sample magnetization usually continues to grow slightly owing to a paraprocess, i.e. the growth of the intradomain magnetization. This growth becomes especially noticeable provided that the temperature is not far below T_C.

The growth of the magnetization after its partial saturation, which is shown by the curves in Fig. 1,*b*, can be attributed to the paraprocess, but only within the temperature interval 270—360 K, because this reason seems improbable for lower temperatures. Therefore, the slow growth of the sample magnetization, which was registered in a wide temperature interval, might indicate that some part of the sample kept its paramagnetic state practically at all temperatures. Under the condition that the fraction of the paramagnetic phase is permanent, this increase would change as T^{-1}. At the same time, in the field range from 2 to 10 kOe, i.e. in the interval where the magnetization, after its partial saturation, reveals a weak growth close to a linear one, its increase does not vary very much, being only slightly reduced as the temperature T decreases. Supposing that the paramagnetic component is responsible for the magnetization growth discussed above, such a behavior can be regarded as resulting from a diminishing of the relative fraction of the sample that remains in the paramagnetic phase as the temperature decreases.

On the other hand, a weak quasilinear growth of the magnetization after its partial saturation is typical of ensembles of particles possessing macroscopically large constant magnetic moments. Their magnetization behavior, e.g., in unidomain particles and superparamagnets, is described by the Langevin function. If this slow increase of the sample magnetization after a partial saturation is a manifestation of the unidomain structure of the particles, it would be only weakened slightly with decrease in temperature, as it has been observed in our case. The best fitting parameters of the Langevin function, which was used for approximating the experimental curves of magnetization, corresponded to the situation where the average magnetic moment of an individual particle became smaller with decrease in temperature, while the number of such particles being increased.

Such a result, at first sight, seems strange. However, the unidomain state of small ferromagnetic particles is realized if the particle sizes are lower than some critical value, which is reciprocal to the intradomain magnetization, or even to its square [2]. At the same time, the intradomain magnetization grows as the

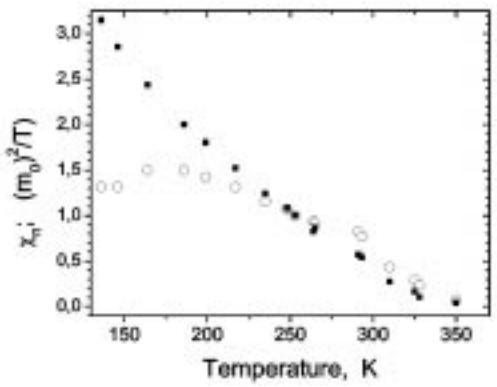

Fig. 2. Temperature dependences of the magnetic susceptibility χ_t (open circles) and the ratio m_0^2/T (solid squares). Both the quantities were normalized by their values at a temperature of 250 K, which is reflected by the subscripts n in the notations on the axis

temperature diminishes. As a result, the number of domains in the zero field and for the given mass of the sample can grow with decrease in temperature. That is, some particles which have a unidomain structure in the vicinity of T_C would be split at a lower temperature into several domains each, and the magnetic moment of the "average" individual domain would diminish. If the intraparticle boundaries of domains should be pinned by the nanoparticle defects, the sample magnetization would occur through the rotation of magnetic moments of those domains. The result would be fairly described by the Langevin function, where the number of Langevin particles and their magnetic moments can change with the temperature. Such a behavior is qualitatively similar to what was observed in our experiments.

However, in the framework of such a consideration, the initial growth of the magnetization before its saturation would become more and more abrupt with decrease in temperature. As a result, the interval of fields, in which the saturation was achieved, would become narrower. But such an effect was not observed. This interval slightly narrows when the temperature is lowered from 360 to 200 K. But its variation was small, or this interval became even extended, with the further lowering of the temperature. One can understand it at a qualitative level as a result of the magnetization of Langevin particles which are characterized by a certain, e.g. uniaxial, anisotropy and possess a random distribution of the anisotropy directions over the ensemble of particles.

The first introduction of the field H usually induces the sample magnetization $M = aH + bH^2 \mathrm{sign} H$ for H smaller or close to the value of the coercive force [2]. In the range of larger fields, which are nevertheless appreciably smaller than the saturation one, there is rather a wide section where the increase dm of the magnetic moment per unit volume of the sample (magnetization) is linear in the increase dH of the magnetic field. So, one may introduce the parameter $\chi = dm/dH$, with $\chi \gg a$. In the large-field part of this section, one can use the approximate relation $m \approx \chi H$. In doing so, the value of χ, calculated from the measurement data obtained for the first, after the sample had been cooled through T_C, introduction of a magnetic field, does not differ much from that calculated after multiple introduction-removal cycles of the field at the same temperature. The "magnetic susceptibility" introduced in such a way for the forced magnetization of a multidomain ferromagnetic sample in the fields that are considerably lower than the saturation one is connected with the mechanism of rearrangement of the magnetization of domains. Its introduction allows the issue concerning the steepness of the dependence of the magnetic moment of a sample on the field in the initial intervals of magnetization to be discussed.

When considering the quantity χ, in order to exclude the influence of the dipole demagnetizing fields which are caused by the external form of the sample, its value is worth recalculating making use of the relation $\chi_t = \chi/(1 - 4\pi N\chi)$. Here, χ_t is the value of the "magnetic susceptibility" induced by the forced magnetization of the sample in the "internal" magnetic field $H_{\mathrm{int}} = H - 4\pi Nm$, and N is the demagnetization factor for the direction of the magnetic field in use.

In Fig. 2, the open circles correspond to the values of the "magnetic susceptibility"which were determined in the manner described above for various temperatures. When plotting the graph, the value $N = 0.08$ was used, which approximately corresponded to the form of the sample used, provided the direction of its magnetization is in the "tablet" plane.

Let us consider the case where the magnetic energy of unidomain particles is comparable with kT, k being the Boltzmann constant. Additionally, we suppose that the "flipping" of the magnetic moments of mechanically fixed particles in an external magnetic field is the main factor of the rearrangement of the multidomain sample state. This "flipping" can be regarded as thermally activated switchings of the magnetic moment directions of unidomain particles over the minima of the magnetic energy, which are defined by both the availability of the equivalent directions for the anisotropy field and the external field. We shall neglect

the paraprocess. In this case, the quantity of the "magnetic susceptibility", which was introduced above in the $H \to 0$ limit and at $T < T_C$, is equal to the sum of two components, $\chi_{H_{\rm int}\to 0} = \chi_T + \chi_O$. Here, χ_T is a contribution to the susceptibility that is proportional to the square of the particle magnetization m_0 divided by the temperature, $\chi_T \propto m_0^2(T)/T$. The value of m_0, if the paraprocess is neglected, is proportional to the temperature-dependent "saturation magnetization" of the sample at a given temperature. And χ_O is a contribution resulted from the canting of the particle magnetization directions from the direction of the anisotropy field towards that of the external magnetic field. If the anisotropy, which prevents the magnetization direction from reorientation, is caused by the anisotropy of the dipole fields that stem from the form of particles, the summand χ_O turns out to be independent of the temperature.

In Fig. 2, the data for the $\chi_t(T)$ dependence (open circles) are exhibited together with the values of the ratio between the square of the "saturation magnetization of the sample at a given temperature" and this temperature (solid squares). The plotted dependences $\chi_t(T)$ and $m_0^2(T)/T$ were normalized by their corresponding values at $T = 250$ K for their comparison to be convenient. One can see that those dependences are very similar in the temperature range above 200 K. But $\chi_t(T)$ starts to lag behind and saturates at lower temperatures. Such a behavior of $\chi_t(T)$ is obviously related to the temperature-independent contribution χ_O to the magnetic susceptibility, with the role of this contribution becoming more and more substantial if the temperature decreases. We note that the linear asymptote of the temperature dependence of $(m_0^2/T)_n$ at $m_0 \to 0$ crosses the temperature axis at $T = 340$ K, which is somewhat lower than T_C. This indicates that one cannot neglect the paraprocess in the vicinity of T_C.

The dependences of the sample magnetic moment, attained at this or that applied magnetic field H_a, on the temperature turned out specific and somewhat different for different kinds of samples (a pressed "tablet" or a powder in the ampoule). While carrying on measurements in the "field-cooling" (FC) mode and at rather small fields, the magnetic moment of a nanopowder consisting of 100–200-nm particles became maximal at a certain temperature below T_C. As the temperature decreased further, the magnetic moment diminished, although insignificantly. The greater was the field, the more weakly this maximum manifested itself and the more its position was shifted towards lower

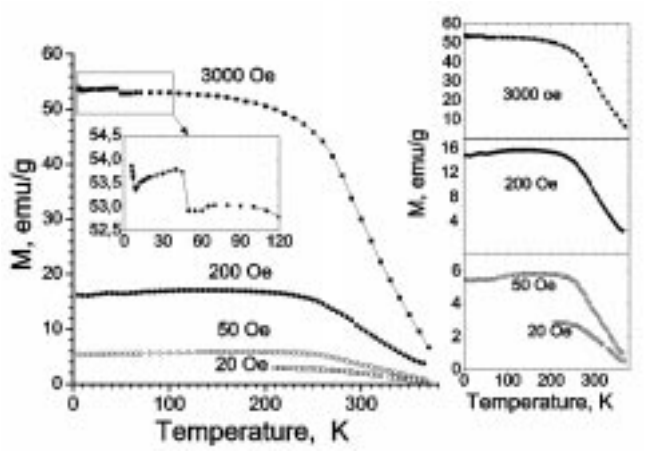

Fig. 3. Temperature dependences of the magnetization of the sample composed of 100—200-nm nanoparticles, measured in various magnetic fields using the FC mode from $T > T_C$ (the left panel). The low-temperature section of the 3-kOe dependence is shown scaled up in the inset. The right panel demonstrates the same dependences on different scales, which makes it possible to confront the dependences for various fields qualitatively

temperatures. For the "tablet" consisting of 50–100-nm particles, the maximum in the $M(T, H = \text{const})$ dependence was practically absent both in small and large fields H. The results of measuring the dependence $M(T, H = \text{const})$ for the powder sample with 100–200-nm particles are shown in Fig. 3. The right panel allows the effect under consideration to be monitored more clearly. Its nature may be attributed to the increase, as the temperature decreases, of anisotropy that opposes to the rotation of the magnetic moment of a unidomain particle (or a domain with pinned boundaries) towards the field direction. But the influence of this phenomenon seemingly should not weaken in a powder with smaller particles. One more discrepancy between the magnetization curves of the samples with different particle sizes is the value of the specific magnetic moment that was achieved at the maximal field of 10 kOe. It turned out larger by approximately 20% in the finer nanopowder. The set of those facts forced us to assume that the observed discrepancies should result merely from the quality of the synthesized substances. The coexistence of ferro- and antiferromagnetic phase domains is typical of "underdoped" manganites. Provided the substance was compositionally nonhomogeneous, a small amount of the antiferromagnetic phase inclusions can be present in the optimally doped $La_{0.7}Sr_{0.3}MnO_3$ as well. It was these inclusions (in different quantities for various samples)

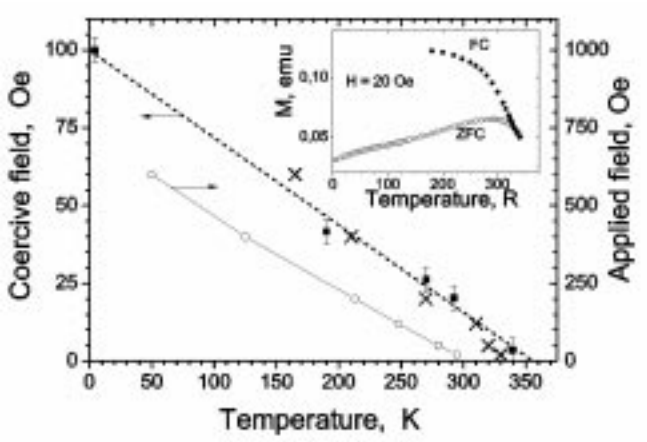

Fig. 4. Temperature dependences of the coercive force of the studied sample (solid squares, the left scale) and the magnetization parameters measured in various fields in the zero field cooling (ZFC) mode: each open circle corresponds to the temperature, at which the temperature dependence of the sample magnetization measured after its ZFC in the given applied field (the right scale) had a maximum; crosses mark the temperatures, at which the dependences measured in the corresponding applied field (the right scale) in the ZFC and FC modes coincided. An example of experimental data concerning the measurements of magnetization in the ZFC and FC modes in a field of 20 Oe is shown in the inset

that might result in the sample magnetization with the maximum at a certain temperature and in a difference of the magnetic moments that were achieved in the field sufficient to make the ferromagnetic part of the sample saturated.

A step-like peculiarity at $T = 44 \pm 2$ K in the dependence $M(T, H = \text{const})$ for a 100–200-nm powder (see Fig. 3) also attracts attention. The similar peculiarity was observed earlier in [3–5]. In [3, 4], this feature was attributed to a magnetic ordering of the impurity phase Mn_3O_4 (with $T_C \approx 42$ K), which might be available in a small amount in the prepared nanopowders. In [5], this feature was connected with the freezing of the spin-glass phase in the surface layers of nanoparticles. In our measurements carried out for various available powder samples, this peculiarity revealed itself with various relative amplitudes but at the same temperature. At the same time, it was absent absolutely for the "tablet". Therefore, the assumption that the impurity phase Mn_3O_4 is responsible for this feature seems more substantiated because the various numbers of small grains of this phase can be presented in various samplings.

The dependence of the coercive force value on the temperature is shown in Fig. 4. One can see that it decreases linearly with the temperature and vanishes near (by 10 ± 5 K below of) T_C. Such dependence is not inherent in the bulk multidomain ferromagnets. However, it can be typical of a superparamagnet in the state below the blocking temperature T_b if we suggest that the barrier height, ΔE, for the reorientation of the particle magnetization from one of the equivalent (without the magnetic field) potential wells to another is proportional to the magnetic moment of the particle M_i: $\Delta E \approx \text{const} \times M_i$. Indeed, if the directions of the particle magnetization in these potential wells are aligned along and against the field correspondingly, the probability (per time unit) of the particle magnetization reorientation from the direction against the field to the direction along it will be determined by the Arrhenius law

$$W = \nu_0 \exp[-(\text{const} M_i - M_i H)/kT], \quad (1)$$

provided that the field has changed its sign in the course of the magnetization cycle from the saturation field to zero and, further, from zero to the saturation field but with the opposite sign. If the "frequency of attempts" ν_0 is rather high, the "coercive force" H_{coer} of the blocked superparamagnetic state can be determined from the condition that the probability of reorientation becomes unity in the mean characteristic "time of observation" t_{obs}, i.e. from the condition $\text{const} \times M_i - M_i H_c \approx kT \ln(\nu_0 t_{\text{obs}})$. In its turn, the condition of blocking will read: $\text{const} \times M_i \approx kT_{\text{b}} \ln(\nu_0 t_{\text{obs}})$. From here, we obtain immediately

$$H_{\text{coer}} \approx \text{const}(1 - T/T_b), \quad (2)$$

which corresponds qualitatively to the experiment. The condition $\Delta E \approx \text{const} \times M_i$, as well as the observed value of $H_{\text{coer}}(T \to 0)$, does not contradict the assumption that "blocking" in the studied system is connected with the mutual dipole-dipole fields of closely located nanoparticles rather than the barriers between the equivalent easy axes of anisotropy. Unfortunately, in this measurement cycle, we did not succeed in measuring the "ensemble of dissolved nanoparticles", where the latter would be separated by non-magnetic spaces in order to exclude their dipole-dipole interaction.

Usually, the routine of studying the magnetostatic properties of ultrasmall magnetic particles includes the measurement of the temperature dependence of the magnetization M in definite small fields. First, the measurement is carried on in the "zero-field cooling" (ZFC) mode; afterwards, a small measuring field H_a is introduced and the dependence $M_{\text{ZFC}}(T, H = H_a)$

is measured, while the sample is being heated up. For a superparamagnet, the maximum in its $M_{\rm ZFC}(T, H = H_a)$ dependence is observed at a certain temperature. At a temperature that is not much higher, the curves $M_{\rm ZFC}(T, H = H_a)$ and $M_{\rm FC}(T, H = H_a)$, measured in the same field H_a in the ZFC and FC modes, respectively, coincide. This temperature is reasonable to be accepted for the temperature of superparamagnetism blocking at the given H_a, $T_{\rm b}(H_a)$. The limit $T_{\rm b}(H_a \to 0)$, measured in various small applied fields in the ZFC mode, should be regarded as the temperature of total superparamagnetism blocking. (Sometimes in the literature, the temperature of the maximum point of $M_{\rm ZFC}(T, H_a \to 0)$ is wrongly recognized as $T_{\rm b}$.) At temperatures below $T_{\rm b}$, the hysteresis does exist, while at higher temperatures, it should be absent.

Our samples also revealed the maxima in their dependences $M_{\rm ZFC}(T, H = H_a)$ for small fields H_a. The larger the field applied to the sample, the lower was the temperature of the maximum. The presence of those maxima, however, was not accompanied by the disappearance of the hysteresis at the temperatures above the point of coincidence of the ZFC and FC curves. Therefore, the maximum points in the $M_{\rm ZFC}(T, H = H_a)$ dependences that were observed in our case, or to put it more exactly, the points close to them, where the ZFC and FC curves coincide, do not correspond to the "blocking" temperatures, but correspond to the temperatures, at which the coercive field attains some value connected with the measuring field H_a through a certain relation. That is, at lower temperatures, there takes place the "blocking" of the domain (unidomain particle) remagnetization owing to coercitivity rather than the blocking of the superparamagnetic state. The examples of the ZFC and FC curves obtained for one of the samples in a field of 20 Oe are shown in the inset in Fig. 4. In the figure itself, the dependence of the temperature of the $M_{\rm ZFC}(T, H = H_a)$ curve maximum on H_a is shown together with the temperature dependence of the coercive field $H_{\rm coer}(T)$. The former dependence is obviously seen to be practically linear as well. It differs from the dependence $H_{\rm coer}(T)$ by a scale factor and is shifted towards lower temperatures. In its turn, the dependence of the temperature, where the $M_{\rm ZFC}(T, H = H_a)$ and $M_{\rm FC}(T, H = H_a)$ dependences coincide (denoted by crosses in the figure), on the applied field H_a can be superimposed on the dependence $H_{\rm coer}(T)$, within the error limits, by multiplying the former by a numerical coefficient. The corresponding numerical coefficient (the ratio of the left and right scale units in the figure) occurred to be 10 ± 0.25.

Therefore, $\lim_{H_a \to 0} T(H_a)$ is attainable only at $T = T_C$. It means that, formally, there was no superparamagnetism within the whole temperature range of ferromagnetic ordering. Taking into account that the coincidence of the $M_{\rm ZFC}(T, H = H_a)$ and $M_{\rm FC}(T, H = H_a)$ dependences is always determined with a standard measurement accuracy, we carried out several special measurements, where both the temperature and the magnetic moment were determined with an enhanced accuracy. It turned out that the ZFC and FC curves came closer to each other and merged with each other asymptotically. That is, as the measurement accuracy increases, so that we might register a smaller and smaller difference between those curves effectively, the defined above "temperature, at which the curves coincide", is revealed closer and closer to T_C.

Thus, the system of $La_{0.7}Sr_{0.3}MnO_3$ nanoparticles, either pressed into a macrosample or packed rather densely with respect to one another, possesses the magnetization of the ferromagnetic type with a hysteresis loop. Such magnetization properties of the nanoparticle ensemble, which are similar to those of the bulk substance, are connected to a great extent with the dipole-dipole interaction between particles. In other respects, the particles behave as independent of one another. This independence manifests itself in the temperature dependence of the sample magnetic susceptibility at the initial stage of rearrangement of its multidomain state under the action of the external magnetic field (a similar rearrangement is expected to take place in superparamagnets) and in the characteristic temperature dependence of the coercive field.

4. EPR/FMR Studies of Nanoparticle Powders

The EPR/FMR studies of nanoparticle powders were fulfilled at a frequency of 9300 MHz and in the temperature range 77—450 K using a Radiopan SEX-2544 spectrometer. Typical records of spectra for a number of temperatures are shown in Fig. 5. It is evident that the EPR line, observed relatively narrow at temperatures above $T_C = 360$ K, becomes broader, mainly on the small-field side, starting from this temperature. Further, it is transformed into a typical spectrum of the ferromagnetic resonance of a powder [6]. It was mentioned above that, while carrying on

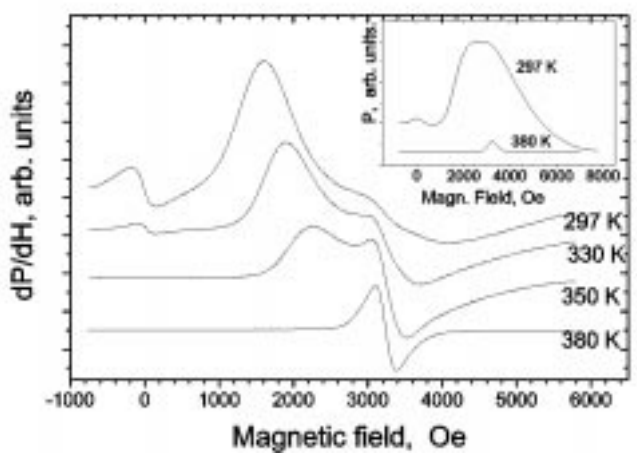

Fig. 5. Records of the EPR/FMR spectra of the $La_{0.7}Sr_{0.3}MnO_3$ powder at various temperatures. The primary EPR/FMR absorption lines at 297 and 380 K, calculated by numerical integration of the registered field derivatives of the absorption, are shown in the inset

EPR/FMR measurements, we used the powder that had not been fixed mechanically in the ampoule, so that the particles, if they were anisotropic, could rotate so that their easy axes of magnetization might align along the magnetic field. Therefore, the observable FMR spectrum should not be considered as the spectrum of an ensemble of particles, whose axes of anisotropy were oriented randomly with respect to the magnetic field direction. The ensemble, at least in part, was grain-oriented. The total anisotropy field in the FMR of an individual particle is governed by the combination of the actual crystallographic magnetic anisotropy and the anisotropy of the demagnetization factor tensor, which is dependent on the form of the particle under consideration [6]. One may expect that the easy axes of the majority of the particles would be aligned along the field. At the same time, the particles of the ensemble have a substantial dispersion of their dimensions and forms. Therefore, the relevant FMR fields of individual particles would be different owing to the dispersion of the total anisotropy, regardless of the alignment of the particles' easy-axes. Under the circumstances, the total anisotropy of the particle ensemble may be of the "easy-axis" type (the total field of anisotropy $H_{A1}^{\text{eff}} > 0$), with the condition

$$2\pi\nu_{\text{res}} = \gamma(H_{\text{res}} + 2H_{A1}^{\text{eff}}) \tag{3}$$

for the FMR to occur, or of the "easy-plane" type ($H_{A1}^{\text{eff}} < 0$), with the relevant condition

$$(2\pi\nu_{\text{res}})^2 = \gamma^2 H_{\text{res}}(H_{\text{res}} - 2H_{A1}^{\text{eff}}) =$$

$$= \gamma^2 H_{\text{res}}(H_{\text{res}} + 2|H_{A1}^{\text{eff}}|), \tag{4}$$

(see [6]).

Expressions (3) and (4) were written down in the approximation, where the constants of anisotropy of the second order only are taken into account and where the total effective field of anisotropy H_{A1}^{eff} is defined as the anisotropy field of a spherical particle. This results in the relationship between the resonance frequency and the resonant field, which is identical to that for a particle of the given form and possessing a certain crystallographic anisotropy. The quantities H_{res}, ν_{res}, and γ in Eqs. (3) and (4) are the resonant field, the FMR frequency, and the gyromagnetic ratio, respectively. In order to analyze the FMR spectra shown in Fig. 5, or similar to them, which have been measured at other temperatures, it is necessary to know the distribution function of the particle's form. This information is absent, and the very procedure of carrying out such an analysis is not trivial. Therefore, we confine ourselves to some estimation. In the case of spindle-shaped particles, the intrinsic crystallographic anisotropy of which is appreciably smaller than the contribution from the anisotropy of demagnetizing fields, the contribution of the latter to H_{A1}^{eff} can amount up to πM. The resonant fields of such particles are described by formula (3). At the same time, for "pancake" particles, the contribution to H_{A1}^{eff} can amount down to $-2\pi M$, and the resonant fields of such particles are described by formula (4). In both the cases, a shift of the FMR line towards smaller fields, as compared with the EPR line at $T > T_C$, should be observed. This corresponds to the experiment. The shift value can be compared quantitatively with the literature data concerning the FMR in the epitaxial $La_{0.7}Sr_{0.3}MnO_3$ film (see, e.g., [7]). In [7], the conclusion was drawn that the intrinsic magnetic crystallographic anisotropy of the film under investigation was negligibly small in comparison with the contribution of the demagnetization factor tensor anisotropy. Returning back to our nanopowders, we may also regard the intrinsic crystallographic magnetic anisotropy of the powder particles insignificant if we suppose the deviations of the particle forms from the spherical one to be rather large (e.g., if the ratio between the maximal and minimal linear sizes of the particle can attain the value of 2—3) and the dependence $M(T_C - T)$ to be the same as in [7].

A remarkable feature of the FMR spectra of the studied nanopowders, when they were measured using the field sweep from a small "negative" value through

the zero point and up to the desirable maximal field, is an extra absorption peak in a narrow region near the zero field. This region corresponds to the remagnetization interval of unidomain particles. The absorption peak in this region testifies to that the microwave magnetic field stimulates thermally activated flips of the magnetization directions of individual nanoparticles between the equivalent "easy" directions, being absorbed at that.

We note that any manifestation, similarly to what was registered in [7], of the extra microwave absorption attributed to the colossal magnetoresistance and the phase transition at T_C (not only from the para- to the ferromagnetic state, but also from the insulator to the metal one), has not been observed in the electron magnetic resonance of the nanopowders. This is surely connected with the fact that separate nanoparticles contact with one another at some places only. As a result, the total resistivity of their ensemble is too high to excite noticeable eddy currents in the ensemble by applying the ac magnetic field of a microwave cavity. The sizes of the particles in our samples were much smaller than the thickness of the skin layer in them. Therefore, the modification of the EPR/FMR line shape, which might be attributed to conductivity, also did not occur.

5. NQR and NMR in the Internal Field of the ^{139}La Nuclei in $La_{0.7}Sr_{0.3}MnO_3$ Nanopowders

One of the methods to study the magnetic and orbital ordering in crystals of manganites is the nuclear magnetic resonance in the internal hyperfine field of magnetically ordered states. In many cases, the objects of investigation (see, e.g., [3] and references therein) are ^{55}Mn nuclei. In this paper, we studied the nuclear resonance of ^{139}La nuclei. They have the spin $I = 7/2$, $\gamma/2\pi = 6.0146$ MHz/T, and the nuclear quadrupole moment $Q = 0.3 \times 10^{24}$ cm^2 [8] (according to the later data, $Q = 0.23 \times 10^{24}$ [9] or 0.22×10^{24} cm^2 [10]).

Earlier, either the NQR/NMR of ^{139}La nuclei in the internal field of the ferromagnet at temperatures below T_C [10–13] or the quadrupole-extended NMR in a strong (up to several T) external magnetic field, shifted by the internal one [10, 12–14], has been observed in $La_{1-x}A_xMnO_3$ polycrystals (where Ca ions played a role of the substituent A, in the main).

The interaction of the nuclear spin levels with both the magnetic field and the intracrystalline electric field gradient (EFG) is described by the Hamiltonian [15]

$$H_N = \hbar\gamma \mathbf{BI} + \frac{h\nu_Q}{6}[3I_z^2 - I(I+1) + \frac{1}{2}\eta(I_+^2 + I_-^2)], \quad (5)$$

where $\nu_Q = 3e^2Qq_{ZZ}/2hI(2I-1)$ is the "quadrupole frequency", $\eta = (q_{XX} - q_{YY})/q_{ZZ}$ is the EFG asymmetry parameter, q_{XX}, q_{YY}, and q_{ZZ} are the principal values of the EFG tensor, I_Z and $I_\pm = I_X \pm I_Y$ are the components of the nuclear spin operator, $\mathbf{B} = \mathbf{B}_{\rm appl} + \mathbf{B}_{\rm hf}$ is the effective magnetic field that affects nuclear spins in magnetically ordered substances, $\mathbf{B}_{\rm appl}$ is the applied external field (corrected, if necessary, by the demagnetization factor of the sample form), and $\mathbf{B}_{\rm hf}$ is the effective hyperfine field proportional to the average value of the spin projections of magnetic ions in the crystal onto the magnetization direction (for ferri- and antiferromagnets, onto the magnetization direction of the sublattices, to which the ions are related). In the structure of the manganite type, the field $\mathbf{B}_{\rm hf}$ is formed by a superhyperfine interaction of La nuclei with 8 nearest neighbor Mn ions. The hyperfine fields of those neighbors are summed up, resulting in the total $\mathbf{B}_{\rm hf}$ close to about 3.5 T at helium temperatures if the sample becomes ferromagnetically ordered, and practically compensate each other provided the ordering is antiferromagnetic [12,13].

The local symmetry of La nuclei in $La_{1-x}A_xMnO_3$ manganites is close to the cubic one. Therefore, in a number of papers (see, e.g., [11, 12]), the EFG was supposed negligibly small at the La nuclei positions. However, in [10,14], the EFG was shown to differ from zero, with $\nu_Q \approx 3.8$ MHz and $\eta \approx 0.94$ for $LaMnO_3$. As some La ions were replaced by Ca ones, the EFG diminished depending on the compound content, and the parameters ν_Q and η acquired the values of 3 MHz and 0.3, respectively. Provided $\nu_Q \neq 0$, the quadrupole splitting of nuclear spin levels must take place even in the absence of the nuclear hyperfine or external magnetic field. Transitions between those levels must result in the NQR of ^{139}La nuclei at $T > T_C$. We do not know a paper, where anybody has managed to register this phenomenon.

If $La_{0.7}Sr_{0.3}MnO_3$ undergoes the paramagnetic insulator—ferromagnetic metal phase transition, the electron spin moments of Mn ions become aligned, and the current carriers coupled with these ions by the carrier—ion exchange interaction become spin-polarized. As a result, provided that either the system of Mn ions is magnetically ordered or the current carriers are spin-polarized, the effective field of the hyperfine interaction proportional to the magnetization of the electron spin

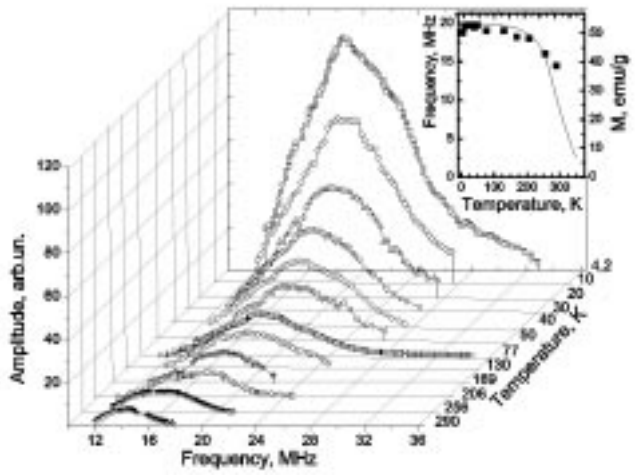

Fig. 6. Temperature dependences of the ^{139}La NQR/NMR spectra in $La_{0.7}Sr_{0.3}MnO_3$. Temperature dependences of the position of the absorption curve maximum (solid squares) and the magnetic moment of the sample in a 3-kOe field (solid curve) are shown in the inset

system of either Mn ions or current carriers, respectively, has to appear at La nuclei. Moreover, the fields of the dipole-dipole interaction of La nuclei with the localized magnetic moments of Mn ions, proportional to the magnetization of the latter, will also be present at them. A combination of those "hyperfine" fields will cause an extra splitting of the nuclear spin states of La. As the temperature diminishes and the spontaneous magnetization of the sample increases, a transition from the limiting case, where the NQR frequency exceeds the splitting of nuclear spin states by the "hyperfine" field of the magnetically ordered compound, to the inverse limiting case has to be observed.

We, as well as the other authors, did not succeed in observing the NQR of ^{139}La nuclei in a $La_{0.7}Sr_{0.3}MnO_3$ nanopowder at $T > T_C$. The most probable reasons of this failure might be a broadening of the NQR line induced by a spatial nonuniformity of the EFG in the solid solution and a sharp reduction of the relaxation times T_1 and T_2 in this temperature range owing to fast fluctuations of the hyperfine field.

In the temperature range below T_C but close enough to it, where the NQR perturbed by the hyperfine field would be observed, the NQR transitions between various quadrupole-split states of spin 7/2 (or the quadrupole satellites of the NMR transition $I_z = 1/2 \leftrightarrow I_z = -1/2$) were not resolved. At the maximal temperature, where the signal was still observable (about 290 K), a single broad line with a maximum at about 14.5 MHz and a half-height width of about 3.5 MHz was observed. As the temperature decreased appreciably lower than T_C, the intensity of this broad line grew, and its maximum was shifted towards higher frequencies, while the width remained almost constant.

We studied the NQR/NMR in the internal field of nanopowders using the method of nuclear spin echo and in the absence of an external magnetic field. An ISSh-2 NQR spin-echo spectrometer was used in the two-pulse spin echo mode ($\pi/2$ and π) (the Khan method). The sample temperature was controlled within the range 4.2—300 K. The durations τ_1 and τ_2 of the pulses, which excited the echo, were longer than 2 μs in our case, i.e. their Fourier spectra were appreciably narrower than the width of the nonhomogeneously broadened line. As a result, our pulses excited rather a narrow spectral package of this line only. The receiver bandwidth of 0.8 MHz was also narrower than the width of the line. Therefore, we registered the response from this spectral package only. Scanning the carrier frequency of the rf pulses in the range of the NQR/NMR line enabled us to reproduce the contour of the studied spectrum. The selection of the amplitudes of exciting pulses for the optimal observation of spin-echo signals showed that, for the durations of pulses indicated above, the supply voltage of a pulse power generator should be reduced by a factor of about 30, in comparison with optimal conditions of the NQR observation in non-magnetic samples in the same frequency range. This evidences for a large (up to several hundreds) enhancement factor of the interaction between the exciting electromagnetic field and the nuclear spin system, which is characteristic of the NMR observations in the internal field of ferromagnetic samples [9].

The plot of the frequency position of spectra at various temperatures, which were obtained in such a manner, is shown in Fig. 6. The dependence of the frequency position of the NQR/NMR line maximum on the temperature is shown in the inset together with the temperature dependence of the saturation magnetic moment M_s which was obtained in a rather large field of 3 kOe. The scales of plots were chosen such that they made the comparison of plots to be convenient. It is evident that the temperature dependence of the maximum of the recorded line turns out proportional, within the limits of measurement errors, to $M_s(T)$ in the temperature interval where the spectra were observed with confidence. This testifies to that the value of ν_Q is low for our sample, being several times lower that the half-width of the line observed. Hence, the frequency of this line was governed by the hyperfine field ($\nu =$

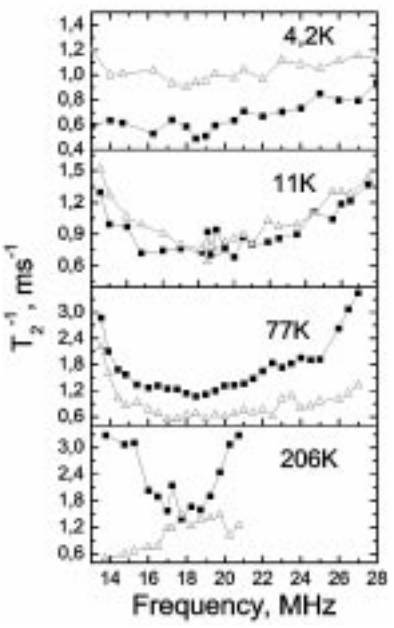

Fig. 7. Dependences of the quantities T_{2q}^{-1} (solid squares) and T_{2m}^{-1} (open triangles) on the position of the carrier frequency of exciting pulses on the line contour for various temperatures

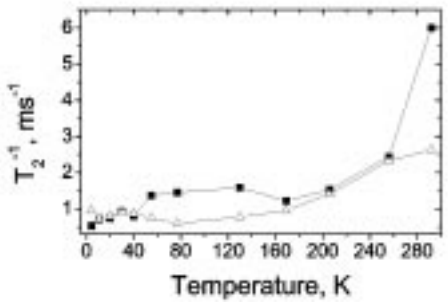

Fig. 8. Temperature dependences of T_{2q}^{-1} (solid squares) and T_{2m}^{-1} (open triangles) at the maximum of the ^{139}La NQR/NMR line

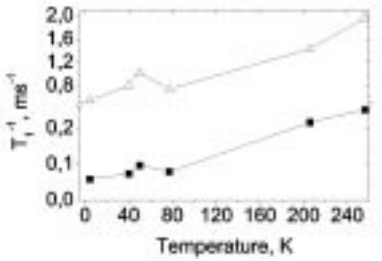

Fig. 9. Components to the longitudinal relaxation rate versus temperature

$= (\gamma/2\pi)\mathbf{B}_{\rm hf}$) within the whole interval of observation. Under the circumstances, an additional reason why we did not achieved a success in observing the NQR/NMR of ^{139}La nuclei at temperatures above 290 K can be a sharp decrease of the average resonance frequency of the NQR/NMR line at higher temperatures, which is expected from the analysis of the plots in the inset in Fig. 6, and the line broadening owing to the dispersion of local T_C values.

The contribution of the quadrupole interaction to the spectrum reveals itself in the character of the transverse (spin-spin) relaxation of T_2. It turns out that the dependence of the spin echo signal decay on the time delay τ between the $\pi/2$ and π exciting pulses is better described by the equation

$$I(\tau) = I_0 \exp\left(-\frac{2\tau}{T_{2q}}\right) \exp\left[-\frac{1}{2}\left(\frac{2\tau}{T_{2m}}\right)^2\right] \qquad (6)$$

than by other approximations. This equation is known in the magnetic resonance theory as that resulting from the presence of nuclear magnetization fluctuations of two types. In the case of the quadrupole-perturbed NMR, the time T_{2q} is related to the EFG fluctuations, and T_{2m} to those of the magnetic interaction. In Fig. 7, the dependences of the relaxation rates T_{2q}^{-1} and T_{2m}^{-1} on the position of the carrier frequency of exciting pulses on the line contour are shown. Fig. 8 exhibits the temperature dependences of T_{2q}^{-1} and T_{2m}^{-1} at the point of the line maximum. As stems from these figures, the process of transverse relaxation caused by EFG fluctuations dominates in the high-temperature range. When scanning along the contour of the resonance line, this contribution is minimal at the line center, which corresponds to the transition $I_z = 1/2 \leftrightarrow I_z = -1/2$ and is amplified symmetrically on the line wings in the field of unresolved quadrupole satellites. As the temperature is decreased, the mechanism of relaxation connected with magnetic fluctuations enhances and at last becomes dominant at temperatures below 10–15 K.

The temperature dependence of the longitudinal relaxation rate, which was obtained from the dependence of the spin echo delay on the time $\tau_{1,2}$ between the pairs of the $\pi/2$ and π pulses, is displayed in Fig. 9. The ratio between the echo amplitudes after the second pair of pulses and the first one is well approximated within the whole temperature interval by the equation that corresponds to the two-exponential process of longitudinal relaxation:

$$\frac{I_2}{I_1} = [1-[a\exp(-\tau_{1,2}/T_1^{(1)})+(1-a)\exp(-\tau_{1,2}/T_1^{(2)})]]. \qquad (7)$$

Here, $\left(T_1^{(1)}\right)^{-1}$ and $\left(T_1^{(2)}\right)^{-1}$ are the weighted contributions to the relaxation rate from two different

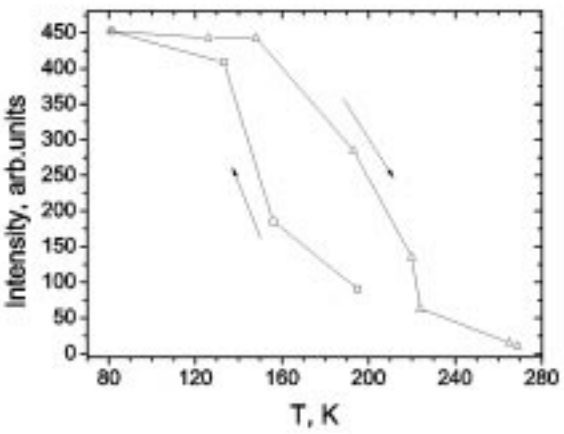

Fig. 10. Temperature dependences of the intensity of the ^{139}La spin echo signal from the demagnetized $La_{0.7}Sr_{0.3}MnO_3$ sample in the ZFC mode from $T > T_C$ and in the course of the following heating

mechanisms, and a and $(1 - a)$ are the fractions of the nuclei that relax according to the first or second mechanism, respectively. From Fig. 9, one can see that the ratio between the rates of those two mechanisms did not vary very much with the temperature, amounting to 9 ± 2. This may indicate that those two processes are related to different relaxational transitions between the nonequidistantly split 7/2-spin sublevels of the ^{139}La nucleus. The relatively insignificant variations of the quantities $\left(T_1^{(1)}\right)^{-1}$ and $\left(T_1^{(2)}\right)^{-1}$ within a rather wide temperature interval most probably testify to that the system of nuclei relaxed to the system of electron spin states rather than to the phonon one.

Fig. 10 exhibits the temperature hysteresis of the intensity of the spin echo signal, which was observed in the mode where the measurements had been started from a high temperature after the sample had been demagnetized (the best way to accomplish it was the sample heating above T_C in a gradually vanishing ac magnetic field (50 Hz)). It is evident that the signal intensity turned out substantially lower in the mode of cooling the sample down to a rather low temperature than that obtained while heating it from some low temperature. It is of interest that if afterwards the sample had not undergone heating to some temperature above T_C, the hysteresis, in the course of the following measurement run accompanied by the sample cooling, reduced and disappeared completely after several similar cycles. We explain the revealed effect by the circumstance that the cooling of the sample to a temperature below that of the superparamagnetic state blocking results in the fixation of the magnetization direction of every particle into a definite direction. The magnetized unidomain particles interact through their dipole fields and, being free for mechanical displacements, stick together into larger conglomerates. During the heating of such conglomerates, they remain stuck together up to the temperature, at which the spontaneous magnetization of particles disappears. The thermally activated reorientation of the magnetization in every of them turns out blocked by the dipole fields of the neighbors. The manifestations of superparamagnetism become weaker or disappear. At the same time, provided that the sample has been heated above T_C and "agitated" with an ac field, the powder particles become separated, and they behave as superparamagnetic ones. The fluctuations of their magnetic moments make impossible the observation of the NMR spin-echo signal from them.

6. Conclusion

While studying the magnetostatic and magnetoresonance properties of the ensembles of $La_{0.7}Sr_{0.3}MnO_3$ nanoparticles that were in the ferromagnetic state owing to the paramagnetic insulator—ferromagnetic metal transition at $T_C = 360$ K, some appearances of the unidomain state of the particles, including those which are typical of superparamagnetism, have been revealed. Those manifestations were modified by the dipole-dipole interaction of nearly located particles in the ensemble. The registered phenomena revealed themselves in peculiarities of the magnetization, the temperature dependence of the coercive force, the FMR zero-field absorption, and the frequency and relaxational characteristics of the quadrupole-perturbed NMR in the hyperfine field of the magnetically ordered state of the particles.

The work was supported in part by the grant VTs/87-297 (the scientific project "Nanophysics and nanoelectronics" of the program "Nanostructure systems, nanomaterials, and nanotechnologies") of the National Academy of Sciences of Ukraine.

1. *Loktev V.M., Pogorelov Yu.G.* // Fiz. Nizk. Temp. — 2000. — **26**. — P. 231.
2. *Vonsovskii S.V.* Magnetism. — Moscow: Nauka, 1971 (in Russian).
3. *Savosta M.M., Krivoruchko V.N., Danilenko I.A. et al.* // Phys. Rev. B. — 2004. — **69**. — P. 024413.

4. *Chen G.J., Chang Y.H., Hsu H.W.* // J. Magn. Magn. Materials. — 2000. — **219**. — P. 317.
5. *Zhu T., Shen B.G., Sun J.R. et al.* // Appl. Phys. Lett. — 2001. — **78**. — P. 3863.
6. *Gurevich A.G.* Magnetic Resonance in Ferrites and Antiferromagnets. — Moscow: Nauka, 1973 (in Russian).
7. *Lyfar D.L., Ryabchenko S.M., Krivoruchko V.N. et al.* // Phys. Rev. B. — 2004. — **69**. — P. 100409(R).
8. *Loshe A.* Kerninduction. — Berlin: Wissenschaften, 1957.
9. *Turov E.A., Petrov M.P.* Nuclear Magnetic Resonance in Ferro- and Antiferromagnets. — Moscow: Nauka, 1969 (in Russian).
10. *Kumagai K., Iwai A., Tomioka Y. et al.* // Phys. Rev. B. — 1999. — **59**. — P. 97.
11. *Dho J., Kim I., Lee S. et al.* // Ibid. — P. 492.
12. *Allodi G., De Renzi R., Licci F., Pieper M.W.* // Phys. Rev. Lett. — 1998. — **81**. — P. 4736 — 4739.
13. *Allodi G., De Renzi R., Guidi G.* // Phys. Rev. B. — 1998. — **57**. — P. 1024.
14. *Allodi G., Cestelli Guidi M., De Renzi R. et al.* // Phys. Rev. Lett. — 2001. — **87**. — P. 127206.
15. *Abragam A.* The Principles of Nuclear Magnetism. — Oxford: Clarendon Press, 1961.

ДОСЛІДЖЕННЯ МАГНІТОСТАТИЧНИХ І МАГНІТОРЕЗОНАНСНИХ ВЛАСТИВОСТЕЙ НАНОПОРОШКІВ $La_{0,7}Sr_{0,3}MnO_3$

О.В. Бондар, В.М. Калита, А.Ф. Лозенко, Д.Л. Лифар, С.М. Рябченко, П.О. Троценко, І.А. Даниленко

Р е з ю м е

Проведено дослідження магнітних та магніторезонансних властивостей наночастинок манганітів $La_{0,7}Sr_{0,3}MnO_3$, розміри яких становлять 50—200 нм. Показано, що зразки намагнічуються подібно до багатодоменних феромагнетиків з петлями гістерезису для всіх температур існування феро фази, а перебудова багатодоменного стану зразка пов'язана з переорієнтацією магнітних моментів однодоменних частинок і має температурну залежність магнітної сприйнятливості у впорядкованому стані, подібну до такої в суперпарамагнетиках. Такий характер намагнічування відповідає перемагнічуванню зразка завдяки термоактивованим перекиданням напрямків намагніченостей окремих однодоменних наночастинок. Це узгоджується також з появою виявленого у феромагнітному резонансі додаткового піка поглинання у вузькій області поблизу нульового поля, де відбувається переорієнтація магнітних моментів наночастинок. Виявлено відмінності у певних особливостях намагнічування зразків, отриманих з наночастинок шляхом механічного пресування, і зразків, де наночастинки знаходяться у стані порошку. Дані ЯКР/ЯМР ядер ^{139}La у внутрішньому полі феромагнітного зразка, отримані для порошків наночастинок $La_{0,7}Sr_{0,3}MnO_3$, також свідчать про прояви суперпарамагнетизму окремих наночастинок разом із впливом диполь-дипольної взаємодії близько розташованих частинок ансамблю, коли однодоменні намагнічені частинки, внаслідок такої взаємодії, утворюють багаточастинкові конгломерати, зв'язані магнітними пондеромоторними силами.

ИССЛЕДОВАНИЯ МАГНИТОСТАТИЧЕСКИХ И МАГНИТОРЕЗОНАНСНЫХ СВОЙСТВ НАНОПОРОШКОВ $La_{0,7}Sr_{0,3}MnO_3$

А.В. Бондарь, В.М. Калита, А.Ф. Лозенко, Д.Л. Лыфарь, С.М. Рябченко, П.А. Троценко, И.А. Даниленко

Р е з ю м е

Проведены исследования магнитных и магниторезонансных свойств наночастиц манганитов $La_{0,7}Sr_{0,3}MnO_3$, размеры которых составляют 50—200 нм. Показано, что образцы намагничиваются подобно многодоменным ферромагнетикам с петлями гистерезиса для всех температур существования феррофазы, а перестройка многодоменного состояния образца связана с вращением магнитных моментов однодоменных частичек и имеет температурную зависимость магнитной восприимчивости в упорядоченном состоянии, подобную таковой для суперпарамагнетиков. Такой характер намагничивания отвечает перемагничиванию образца благодаря термоактивированным перебросам направлений намагниченностей отдельных однодоменных наночастиц. Это согласуется также с появлением обнаруженного в ферромагнитном резонансе дополнительного пика поглощения в узкой области вблизи нулевого поля, где происходит переориентация магнитных моментов наночастиц. Выявлены отличия в ряде особенностей намагничивания образцов, полученных из наночастиц путем механического прессования, и образцов, где наночастицы находятся в состоянии порошка. Данные ЯКР/ЯМР ядер ^{139}La во внутреннем поле ферромагнитного образца, полученные для порошков наночастиц $La_{0,7}Sr_{0,3}MnO_3$, также свидетельствуют о проявлении суперпарамагнетизма отдельных наночастиц вместе с влиянием диполь-дипольного взаимодействия близко расположенных частичек ансамбля, когда однодоменные намагниченные частички вследствие такого взаимодействия образуют многочастичные конгломераты, связанные магнитными пондеромоторными силами.